

Interference effects in photodetachment of F^- in a strong circularly polarized laser pulse

S. Bivona, G. Bonanno, R. Burlon,^{*} and C. Leone

*Dipartimento di Fisica e Tecnologie Relative, Università degli Studi di Palermo, Palermo, Italy
and CNR-CNISM, Viale delle Scienze, Edificio 18, I-90128 Palermo, Italy*

(Received 25 May 2007; published 30 August 2007)

A numerical simulation of photodetachment of F^- by a circularly polarized laser pulse has been accomplished by using a Keldysh-type approach. The numerical results are in agreement with measurements of photoelectron energy spectra recently reported in the literature. The features exhibited by the spectra are traced back to quantum interference effects, in the same spirit as in a double-slit experiment in the time domain.

DOI: [10.1103/PhysRevA.76.021401](https://doi.org/10.1103/PhysRevA.76.021401)

PACS number(s): 32.80.Rm, 32.80.Gc

Recent developments in laser technology have made it possible to produce short, high-power laser pulses with durations of a few optical cycles, which have become available as research tools [1]. For not too short pulses, the electric field may be represented as a product of a monochromatic carrier wave and a positive-definite envelope function. One of the parameters characterizing this type of pulse is the so-called carrier-envelope relative phase. By varying this parameter, the temporal shape of the pulse may vary significantly, allowing coherent control and study of elementary atomic processes. An instance of application of this source to the study of quantum fundamental processes was recently given in attosecond double-slit experiments in the time-energy domain [2]. In these experiments, due to the highly nonlinear processes, the ionization occurs in time windows having a duration of attoseconds. By changing the relative carrier-envelope phase, the temporal shape of the field may be altered in such a way that the time windows may be “open” or “closed”, controlling the recorded photoelectron spectra modulations which can be described in terms of quantum interference.

In order to describe the ionization of an atomic system irradiated by strong laser fields, different nonperturbative methods have been developed [3–10]. The strong-field approximation [3–5] is one of the most widely used models because of its analyticity. The main assumption of this approximation is that the action of the ionic Coulomb field on the photoelectron may be neglected with respect to the driving effect of the laser field, and, therefore, the final electron state may be described by a Volkov wave function. This treatment is believed to describe more accurately the photodetachment of negative ions, because of the short-range nature of the interaction between the photodetached electron and the parent atom.

By using a saddle-point method, Gribakin and Kuchiev [6] have given an analytical solution to the problem of multiphoton detachment by a monochromatic linearly polarized laser field, and have shown that the rapid oscillations in the angular distribution of the n -photon detachment rate may be described in terms of interference of two classical trajectories leading to the same final electron state.

In Ref. [11], Beiser *et al.* extended the approach of Grib-

akin and Kuchiev to the multiphoton detachment of a negative ion by a monochromatic circularly polarized field. By a saddle-point analysis of the transition amplitude they inferred that quantum interference effects do not occur in the direct process of photodetachment by a circularly polarized laser field. Recently, an image technique has been used to measure the energy- and angle-resolved spectrum of electrons produced by the photodetachment of F^- exposed to a circularly polarized infrared femtosecond laser field [12]. The image processing involves a conventional Abel inversion routine, which requires that the electrons be emitted symmetrically with respect to the axis perpendicular to the static electric field that projects the photoelectrons in the (x, z) plane [13], z being the propagation pulse direction. We remark that, while electron emission caused by a monochromatic circularly polarized laser field is expected to be symmetrically distributed around the pulse propagation direction, the azimuthal symmetry breaks down when electrons are detached by short laser pulses. In fact, because during its rotation the electric field amplitude varies, the electron distribution turns out to depend on the azimuthal angle ϕ between the component of the electron momentum \mathbf{q} parallel to the laser polarization plane and the axis along which the electric field reaches its maximum value. However, below we will show that the ejected electron distribution anisotropy is strongly reduced when the spatial distribution of the laser pulse intensity is taken into account, restoring the requirement for using the above-mentioned experimental technique. Of course, in order to understand the features of the recorded electron energy spectra, it is of crucial importance to include the temporal and spatial laser intensity distribution in the simulation. The experimental results show that the angular distribution of the electrons ejected at a given energy, as a function of the angle ϑ between the photoelectron emission direction and the laser pulse propagation direction, does not exhibit any structure that can be associated with quantum interference effects. Instead, the energy distribution of photoelectrons emitted in the polarization plane exhibits structures whose origin has not yet been discussed. The aim of this Rapid Communication is to show that the experimental electron energy spectra exhibit features surviving the damping effects of the laser spatial inhomogeneity that can be explained in terms of quantum interferences. The simulation of the experimental data will be performed by using the Keldysh theory modified to include the shape of the laser

^{*}burlon@unipa.it

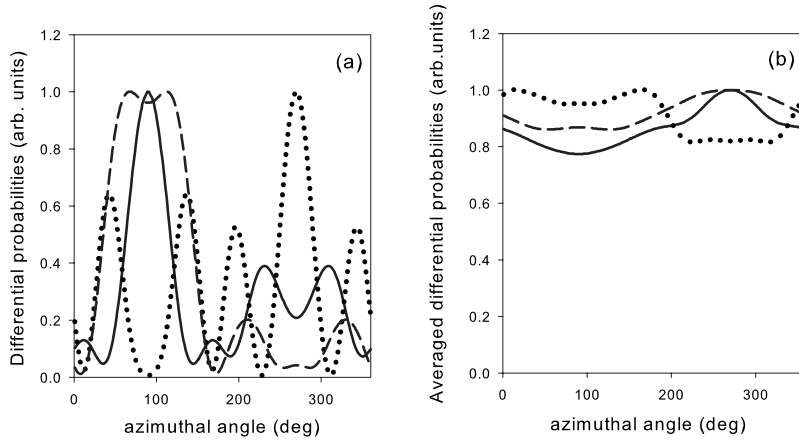


FIG. 1. Photoelectron angular distribution in the (x,y) polarization plane of the laser pulse, calculated (a) by Eq. (5); (b) by Eq. (5) after averaging over the spatial intensity in the laser focus, for three different values of the photoelectron energy ϵ_q . Full line, $\epsilon_q=5$ eV; dotted line, $\epsilon_q=3$ eV; dashed line, $\epsilon_q=7.5$ eV. The field strength E_0 at the laser peak intensity is $E_0=0.032$ a.u., $\omega=0.030$ a.u., $n_c=40$. Each curve has been normalized to its highest value.

pulse [14–16]. In particular, in order to account for the finite duration of the laser pulse, our results will be obtained through calculations of photodetachment probabilities rather than photodetachment rates based on the quasienergy approach, which presupposes the presence of a monochromatic laser field. Within the theoretical approach of Refs. [14–16], Milosevic *et al.* [15] explained the different features of the probability of electron emission into two opposite directions, observed in a stereo above-threshold ionization experiment (ATI) with a few-cycle circularly polarized laser pulse [17]. Let us assume a circularly polarized laser pulse having the electric field

$$\mathbf{E}(t) = (E_0/\sqrt{2})f(t)(\hat{x} \cos \omega t + \hat{y} \sin \omega t). \quad (1)$$

E_0 is the field strength, ω the laser carrier frequency, and $f(t)$ the envelope function. For $f(t)$ we use

$$f(t) = \cos^2(\pi t/\tau)\Theta(\pi/2 - |t|), \quad (2)$$

where τ is the total pulse duration, $\Theta(x)$ is the Heaviside function, and $t=0$ corresponds to the middle of the pulse. In order to have an integer number of cycles we assume $\tau=n_c T$, with $T=2\pi/\omega$ the period of the carrier. The polarization plane is assumed to coincide with the (x,y) plane. The vector potential taken, in Gaussian units, as $\mathbf{A}(t)=-c\int_{-\pi/2}^t dt' \mathbf{E}(t')$, turns out to be zero for $t \leq -\tau/2$ and $t \geq \tau/2$. By assuming that the negative ion is initially in a bound state $\psi_i(r,t)=\psi_i(r)\exp(-iI_0 t)$, the transition amplitude at time t for detachment into the final state $\psi_f(r,t)$, described by a Volkov state with momentum \mathbf{q} , when the laser is off, is given by

$$T_{fi}(t) = -i \int_{-\tau/2}^t dt' \langle \psi_f(\mathbf{r},t') | \mathbf{r} \cdot \mathbf{E}(t') | \psi_i(\mathbf{r}) \rangle \exp\{iS(t')\}, \quad (3)$$

where $\psi_f(\mathbf{r},t)$ is the plane wave describing the photoelectron having an instantaneous momentum $\boldsymbol{\pi}(t)=\mathbf{q}+\mathbf{A}(t)/c$, and $S(t)$ is the combined classical action of the initial and final electron states, whose explicit form is given by

$$S(t) = \int dt' \left(\frac{\boldsymbol{\pi}^2(t')}{2} + I_0 \right). \quad (4)$$

In our calculations $\psi_i(r)$ is approximated by $\psi_i(\mathbf{r})=A r^{-1} \exp(-kr) Y_{l,m}(\hat{\mathbf{r}})$, with A the normalization coefficient, $Y_{l,m}(\hat{\mathbf{r}})$ a spherical harmonic, and l,m the angular momentum numbers of the electron in the initial state, with the quantization axis taken along the propagation direction of the laser pulse. $I_0=-k^2/2$ is the energy of the initial bound state. We note that, for $t \geq \tau/2$, $\mathbf{A}(t)=\mathbf{0}$. Consequently, $\boldsymbol{\pi}(t)=\mathbf{q}$, and the photoelectron kinetic energy ϵ_q may be expressed as $\epsilon_q=q^2/(2m)$. By using Eq. (3), evaluated at the end of the laser pulse ($t=\tau/2$), the differential probability of electron ejection in the solid angle $d\Omega=\sin \theta d\theta d\phi$ and in the energy interval between ϵ_q and $\epsilon_q+d\epsilon_q$ may be written as

$$d\mathcal{P}/(d\Omega d\epsilon_q) = |T_{fi}(t/2)|^2 \sqrt{2\epsilon_q}. \quad (5)$$

In Fig. 1(a) we show the probability of electron emission in the laser polarization plane (x,y) , for three different values of the photoelectron energy, by evaluating Eq. (5) at $\theta=\pi/2$. In order to simulate the experimental conditions reported in Ref. [12], we have taken $E_0=0.032$ a.u., and $\omega=0.030$ a.u., and $n_c=40$. The calculation involves summation of photodetachment probabilities for different values $m=0$ and $m=\pm 1$ of the magnetic quantum number characterizing the initial state of the active electron, and statistical averaging over the detachment channels associated with the two spin-orbit sublevels $P_{1/2}$ and $P_{3/2}$. In Fig. 1(b) are shown the photoelectron distributions obtained by averaging Eq. (5), taken at $\theta=\pi/2$, over the spatial intensity in the laser focal region, which is assumed to have a Gaussian form with focal parameters near to those estimated in Ref. [12] and peak intensity equal to that used when the laser pulse is assumed to be homogeneous. As anticipated above, we observe that, when the laser pulse is spatially homogeneous, the calculated electron distributions are not symmetric with respect to the laser propagation direction. By averaging the results shown in Fig. 1(a) over the spatial distribution of the laser intensity, the electron angular distributions in the laser polarization plane, at a given energy, turn out to be essentially isotropic, as shown in Fig. 1(b). In Fig. 2 we compare the experimental energy distributions of the electrons emitted in the polarization plane, reported in Ref. [12], with our predictions obtained by averaging Eq. (5), evaluated at $\phi=0$ and $\theta=\pi/2$, over the laser spatial intensity in the laser focus at the same laser parameters as in Fig. 1. The experimental

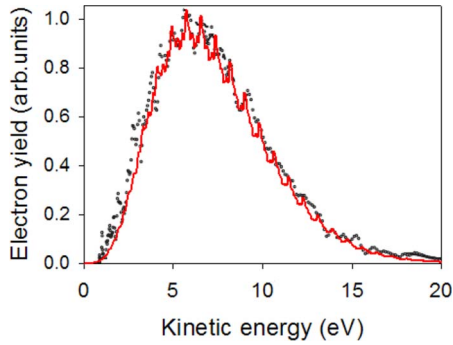


FIG. 2. (Color online) Experimental energy distribution (Ref. [12]) of photoelectrons emitted in the polarization plane (dots) compared to the theoretical predictions obtained by averaging Eq. (5), evaluated at $\phi=0$ and $\theta=\pi/2$, over the spatial laser intensity. Laser parameters as in Fig. 1.

results are reproduced with accuracy, provided the calculations are carried out at the laser peak intensity, which is approximately 35% higher than the measured value. We remark that the estimated precision of the measurement was of the order of 15%, and that previous calculations carried out in Ref. [12] at peak intensity approximately 45% higher than the measured value do not reproduce the structure observed in the experimental data. Finally, we note that, in order to obtain a better agreement between our simulation and the experimental data, we have shifted the zero of experimental energy of the photoelectrons by approximately 0.7 eV. We observe that the experimental determination of this zero might be affected, in the circular polarization experiment, by the circumstance that a large number of electrons are ejected along the direction of the projecting static electric field, so that, at the center of the image ($x=z=0$), in addition to electrons with zero energy, photoelectrons having larger energy are recorded too. In the way, this shift is inessential in explaining the energy spectrum structures. In order to get more insight into this structure, let us consider the sequence of functions $T(n)$ obtained by evaluating the integral giving the transition amplitude over the successive time intervals $[-nT/2, nT/2]$ with $n=1, 2, \dots, n_c$, and assuming \mathbf{q} directed along the x direction,

$$T(n) = -i \int_{-nT/2}^{nT/2} dt \langle \psi_f(\mathbf{r}, t) | \mathbf{r} \cdot \mathbf{E}(t) | \psi_i(\mathbf{r}) \rangle \exp\{iS(t)\}. \quad (6)$$

By using the saddle-point method, $T(n)$ is obtained as

$$T(n) = -i \sum_s [2\pi i \ddot{S}(t_s)]^{1/2} \times \langle \psi_f(\mathbf{r}, t_s) | \mathbf{r} \cdot \mathbf{E}(t_s) | \psi_i(\mathbf{r}) \rangle \exp\{iS(t_s)\}, \quad (7)$$

where the summation is over all n saddle points t_s with $-nT/2 < \text{Re}(t_s) < nT/2$ and $\text{Im}(t_s) > 0$ that are solutions of the equation $\pi^2(t)/2 + I_0 = 0$. Figure 3(a) shows $|T(n)|^2$ as a function of the photoelectron energy for $n=1, 2, 4$. The curve showing $|T(1)|^2$ does not exhibit any structure, as only a single saddle point contributes to its determination. For $n=2$ or 4, both $|T(n)|^2$ show interference effects originating

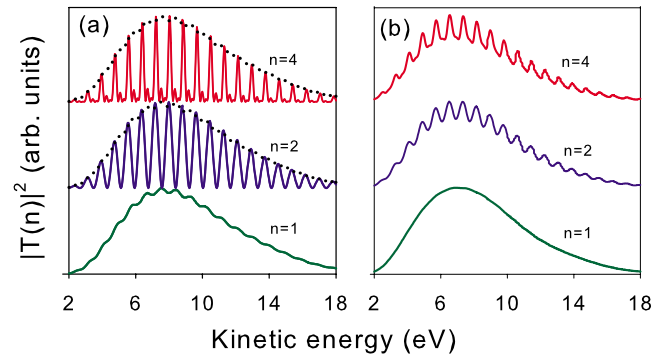


FIG. 3. (Color online) Sequence $|T(n)|^2$ evaluated by integrating the transition amplitude over one (green curve), two (blue curve), and four (red curve) cycles during, respectively, the intervals $[-T/2, T/2]$, $[-T, T]$, and $[-2T, 2T]$ (a) without and (b) with the pulse inhomogeneity taken into account. Laser parameters as in Fig. 1.

from the sum of terms evaluated that correspond to saddle points whose real part is located at points belonging to consecutive laser pulse cycles, such that $\omega[\text{Re}(t_{s+1}) - \text{Re}(t_s)] = 2\pi$. This curves show typical two- or four-slit interference patterns, whose envelope coincides with the curve $|T(1)|^2$, which plays the role of a diffraction function. In fact, we observe that for $n \ll n_c$ the envelope function $f(t)$ defined by Eq. (2) may be put equal to 1 and $|T(n)|^2$ becomes

$$|T(n)|^2 = |T(1)|^2 (\sin^2 n\pi\Delta / \sin^2 \pi\Delta) \quad (8)$$

with $\Delta = (q^2/2 + E_0^2/4\omega^2 + |I_0|)/\omega$. On increasing the number n , the functions $|T(n)|^2$ exhibit an n -slit interference pattern with the principal maxima located at essentially the same electron energy found for $n=2$. Just as occurs in light diffraction by diffraction gratings, on increasing n , the maxima become more sharp and pronounced; moreover, between two consecutive maxima separated by $\hbar\omega$, secondary maxima occur whose number increases with n . We note that, in the limit $n_c \rightarrow \infty$, the results of photodetachment by a monochromatic field are recovered. Figure 3(b) shows the effect of averaging over the spatial laser inhomogeneity. According to the features of the curves reported in Fig. 3, the effect of the spatial

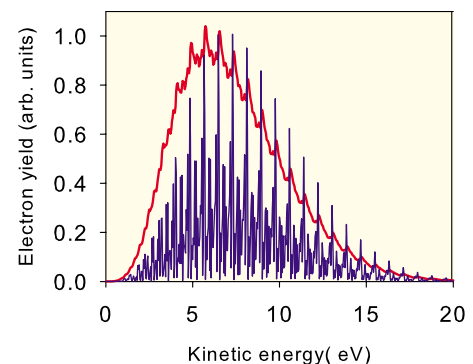


FIG. 4. (Color online) Photoelectron energy spectra calculated by assuming homogeneous [blue (lower) curve] and inhomogeneous [red (upper) curve] pulse. Laser parameters as in Fig. 1.

inhomogeneity of the pulse is to damp the secondary maxima and to shift the absolute maximum to smaller energies. These effects become more pronounced on increasing n . In Fig. 4 we show the effect of the laser inhomogeneity on the photoelectron spectra, taking $n=n_c=40$ corresponding to the total duration of the pulse. We remark that, for the laser parameters used in our simulation, while the highest- and the lowest-energy peaks are almost canceled out, the central region of energy spectra still shows structures that survive the washing-out averaging effect of the spatial laser inhomogeneity. Moreover, the maxima of the oscillations are located at almost the same values of the energies found when the simulation is carried out by assuming a homogeneous field. Therefore, we conclude that the structures exhibited by the experimental energy spectra originate in interference effects. We note that our treatment differs from that used in Refs. [11,12,18] in that, in the approach we follow, the photodetachment probability is first calculated taking into account the temporal pulse shape [19], and then averaging over the spatial laser inhomogeneity; in the other treatment the quan-

tity to be averaged over the spatial and temporal laser inhomogeneities is a photodetachment rate (not a probability) calculated as if the laser field were monochromatic. As a matter of fact, while, on the whole, quite similar results are obtained, the two treatments lead to results that may differ in some details. Note that in our analysis the finite resolution of the detector used in the experiment, which also broadens the peaks [18], has not been taken into account. In conclusion, we have shown that in the framework of a Keldysh-type treatment, by using adjustable parameters describing the laser spatial inhomogeneity, it is possible to trace back the origin of the features shown in recorded photodetachment electron energy spectra to interference effects, in the same spirit as the recently reported double-slit interference in the time domain.

This work was supported in part by the Italian Ministry of University and Scientific Research through the PRIN “Nanostructures Photodeposition for Nonlinear Optics” Grant No. 2004023130.

-
- [1] T. Brabec and F. Krausz, *Rev. Mod. Phys.* **72**, 545 (2000); R. Kienberger *et al.*, *Nature (London)* **427**, 817 (2004).
 [2] F. Lindner *et al.*, *Phys. Rev. Lett.* **95**, 040401 (2005).
 [3] L. V. Keldish, *Sov. Phys. JETP* **20**, 1307 (1964).
 [4] F. H. M. Faisal, *J. Phys. B* **6**, L89 (1973).
 [5] H. R. Reiss, *Phys. Rev. A* **22**, 1786 (1980).
 [6] G. F. Gribakin and M. Yu. Kuchiev, *Phys. Rev. A* **55**, 3760 (1997).
 [7] A. Lohr, M. Kleber, R. Kopold, and W. Becker, *Phys. Rev. A* **55**, R4003 (1997).
 [8] W. Becker *et al.*, *Adv. At., Mol., Opt. Phys.* **48**, 35 (2002).
 [9] B. Borca, M. V. Frolov, N. L. Manakov, and A. F. Starace, *Phys. Rev. Lett.* **87**, 133001 (2001); **88**, 193001 (2002).
 [10] M. V. Frolov, N. L. Manakov, E. A. Pronin, and A. F. Starace, *Phys. Rev. Lett.* **91**, 053003 (2003).
 [11] S. Beiser, M. Klaiber, and I. Y. Kiyani, *Phys. Rev. A* **70**, 011402(R) (2004).
 [12] B. Bergues, Y. Ni, H. Helm, and I. Y. Kiyani, *Phys. Rev. Lett.* **95**, 263002 (2005).
 [13] R. Reichle, H. Helm, and I. Y. Kiyani, *Phys. Rev. Lett.* **87**, 243001 (2001).
 [14] S. X. Hu and A. F. Starace, *Phys. Rev. A* **68**, 043407 (2003).
 [15] D. B. Milosevic, G. G. Paulus, and W. Becker, *Phys. Rev. Lett.* **89**, 153001 (2002); *Laser Phys.* **13**, 948 (2003).
 [16] S. Bivona, R. Burlon, and C. Leone, *Opt. Express* **14**, 12576 (2006).
 [17] G. G. Paulus, F. Grasbon, H. Walter, P. Villorresi, N. Nisoli, S. Stagira, E. Priori, and S. Silvestri, *Nature (London)* **414**, 182 (2002).
 [18] B. Bergues, Z. Ansari, D. Hanstorp, and I. Y. Kiyani, *Phys. Rev. A* **75**, 063415 (2007).
 [19] Study of the effect of envelope functions and finite time on the resolution of spectra has a long history; e.g., E. J. Heller, *J. Chem. Phys.* **68**, 3891 (1978).